Eur. Phys. J. B **13**, 421–427 (2000)

THE EUROPEAN PHYSICAL JOURNAL B

EDP Sciences

Density-matrix renormalization study of the Hubbard model on a Bethe lattice

M.-B. Lepetit, M. Cousy, and G.M. Pastor

Laboratoire de Physique Quantique[a], IRSAMC, 118 route de Narbonne, 31062 Toulouse Cedex 4, France

Received 8 February 1999 and Received in final form 14 June 1999

Abstract. The half-filled Hubbard model on the Bethe lattice with coordination number $z = 3$ is studied using the density-matrix renormalization group (DMRG) method. Ground-state properties such as the energy per site E, average local magnetization $\langle \hat{S}_z(i) \rangle$, its fluctuations $\langle \hat{S}_z(i)^2 \rangle - \langle \hat{S}_z(i) \rangle^2$ and various spin correlation functions $\langle \hat{S}_z(i)\hat{S}_z(j) \rangle - \langle S_z(i) \rangle \langle S_z(j) \rangle$ are determined as a function of the Coulomb interaction strength U/t. The local magnetic moments $\langle \hat{S}_z(i) \rangle$ increase monotonically with increasing Coulomb repulsion U/t showing antiferromagnetic order between nearest neighbors $[\langle \hat{S}_z(0) \rangle \simeq -\langle \hat{S}_z(1) \rangle]$. At large U/t, $\langle \hat{S}_z(i) \rangle$ is strongly reduced with respect to the saturation value 1/2 due to exchange fluctuations between nearest neighbors (NN) spins $[|\langle S_z(i) \rangle| \simeq 0.35$ for $U/t \to +\infty]$. $\langle S_z(i)^2 \rangle - \langle S_z(i) \rangle^2$ shows a maximum for $U/t = 2.4$–2.9 that results from the interplay between the usual increase of $\langle S_z(i)^2 \rangle$ with increasing U/t and the formation of important permanent moments $\langle S_z(i) \rangle$ at large U/t. While NN sites show antiferromagnetic spin correlations that increase with increasing Coulomb repulsion, the next NN sites are very weakly correlated over the whole range of U/t. The DMRG results are discussed and compared with tight-binding calculations for $U = 0$, independent DMRG studies for the Heisenberg model and simple first-order perturbation estimates.

PACS. 71.10.Fd Lattice fermion models (Hubbard model etc.) – 75.10.Lp Band and itinerant models

1 Introduction

Bethe lattices or Cayley trees have often been the basis of very attractive models for the theoretical study of various properties of solids. A Bethe lattice is completely characterized by the number of nearest neighbors z and by the lack of closed loops. The later feature simplifies calculations considerably allowing in many cases to obtain useful insights on the physics of complex problems, for example, in the theory of many electron systems or in the theory of alloys and other disordered systems. Recently, the interest in the study of strongly correlated fermions on Bethe lattices has been renewed by the advances achieved in the limit of infinite spatial dimensionality ($d \to \infty$) [1]. Indeed, this lattice provides a systematic mean of realizing the $d = \infty$ limit by letting $z \to \infty$ and by scaling the nearest neighbor (NN) hopping integrals as $t = W/(4\sqrt{z})$, where W refers to the band width. In this context, an important research effort has been dedicated to the half-filled Hubbard model. This concerns mainly the metal-insulator transition within the paramagnetic phase but also the properties of the antiferromagnetic (AF) phase which in the absence of frustrations is the most stable solution at low temperatures (bipartite lattice) [2–4]. Therefore, it would be of considerable interest to determine the properties of the half-filled Hubbard model on a Bethe lattice with finite z by using accurate numerical methods. Even though the computational effort increases extremely rapidly with z, such numerical studies could be very useful, particularly in view of comparing them with $z = \infty$ results including $1/z$ corrections.

The aim of this paper is to determine several ground-state properties of the half-filled Hubbard model on a $z = 3$ Bethe lattice as a function of the Coulomb interaction strength U/t. For this purpose we take advantage of a property that Bethe lattices share with one-dimensional (1D) chains, namely, the fact that there is only one path between any pair of sites in the system. This characteristic allows the design of a simple real-space renormalization scheme in order to apply the density-matrix renormalization group (DMRG) method [5]. Density-matrix renormalization is a very powerful technique which was proposed a few years ago in the context of 1D spin systems. Since then it has been rapidly extended to become one of the leading numerical tools for the study of low-dimensional correlated quantum systems, including recently two-dimensional lattices of finite size [6]. The success and wide range of applications found by this approach rely on two main qualities: its high accuracy even for systems as large as a few hundreds of sites, which allows safe extrapolations to the thermodynamic limit, and its flexibility concerning the model Hamiltonian under study (Heisenberg, t-J,

[a] UMR 5626 du CNRS

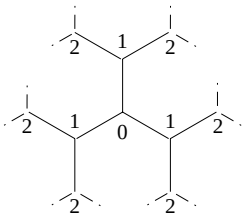

Fig. 1. Illustration of the Bethe lattice with coordination number $z = 3$. The numbers label non-equivalent sites.

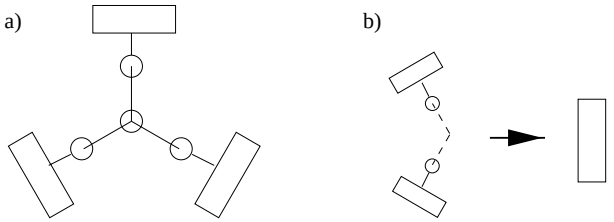

Fig. 2. (a) Renormalized Bethe lattice ($z = 3$, see Fig. 1) and (b) renormalization procedure ($\nu \geq 3$). Circles represent sites which are treated exactly and rectangles represent renormalized blocks. Notice that the total number of sites $N_{\rm a} = 3\times 2^{\nu}-2$ increases exponentially with the number of renormalization iterations ν.

Hubbard, Kondo, etc). However, except for works on the spin-1/2 XXZ and Heisenberg Hamiltonians [7], the infinite DMRG calculations have always been limited to 1D problems. To our knowledge, this is the first time that the DMRG algorithm for infinite systems is applied to a fermion model not having the 1D topology.

The remainder of the paper is organized as follows. In the next section the main details of the application of the DMRG method to the Bethe lattice are given. Results for the ground-state energy and several spin and charge local properties are presented and discussed in Section 3. Finally, Section 4 summarizes our conclusions.

2 Details of the calculation

We consider the Hubbard Hamiltonian [8]

$$H = -t \sum_{\langle i,j\rangle,\sigma} \hat{c}^{\dagger}_{i\sigma}\, \hat{c}_{j\sigma} \;+\; U \sum_{i} \hat{n}_{i\uparrow}\, \hat{n}_{i\downarrow} \qquad (2.1)$$

on a Bethe lattice with coordination number $z = 3$ (see Fig. 1). In the usual notation, $\hat{c}^{\dagger}_{i\sigma}$ ($\hat{c}_{i\sigma}$) creates (annihilates) an electron with spin σ at site i, $\hat{n}_{i\sigma} = \hat{c}^{\dagger}_{i\sigma}\hat{c}_{i\sigma}$ is the number operator, t refers to the nearest neighbor (NN) hopping integral, and U to the on-site Coulomb repulsion. Several ground-state properties of the Hubbard model are determined using the DMRG method [5]. This is an iterative projection technique which allows to include the most relevant part of the ground-state wave function on a limited number of many-body states. The system is partitioned into several regions in real space or blocks, between which renormalized interactions are computed. The accuracy of the method is controlled by the number of states m retained for the description of each block. In the DMRG algorithm for infinite systems, the size of the system is increased at each renormalization step and the properties of the thermodynamic limit are determined by extrapolating the succession of finite system calculations.

The renormalization procedure used for the $z = 3$ Bethe lattice is illustrated in Figure 2. Starting from a central site $i = 0$ and the two shells of its first and second NN's, a new shell of NN's is added at each iteration ν. The total number sites is thus given by $N_{\rm a} = 3 \times 2^{\nu} - 2$. Notice the contrast with the usual DMRG scheme for 1D systems [5] where $N_{\rm a}$ increases linearly with ν. The central site and its NN's (the sites on the first shell) are treated exactly at all iterations and the renormalizations are performed on the two branches that start at each of the first-shell sites. The DMRG step treats two renormalized blocks plus two sites as the system block, leaving the remaining block and two sites as environment block (see Fig. 2). Notice that no renormalization is actually done until $\nu = 3$, *i.e.*, the 10-site system with two sites in each block is treated exactly. In practice, the extrapolations of the considered properties to $\nu \to \infty$ converge after $\nu \simeq 15$ iterations. At this point $N_{\rm a} \simeq 2 \times 10^5$. It should be however noted that in a Bethe lattice the surface to volume ratio does not vanish with increasing number of shells L. Taking into account that the number of sites in the lth shell is $N_{\rm s} = z(z-1)^{l-1}$ ($l \geq 1$), one finds for $z = 3$ that 1/2 of the sites belong to the outermost shell, 1/4 to the first shell below the surface, 1/8 to the second shell below the surface and so forth. Consequently, global properties of the system such the average ground-state energy per site $E_{\rm s}$ are dominated by the outermost shells. Bulk properties corresponding to the translational invariant situation have to be calculated locally. For instance, the ground-state energy per site E is determined from $E = U\langle \hat{n}_{0\uparrow}\hat{n}_{0\downarrow}\rangle + (zt/2)\sum_{\sigma}\langle \hat{c}^{\dagger}_{1\sigma}\hat{c}_{0\sigma} + \hat{c}^{\dagger}_{0\sigma}\hat{c}_{1\sigma}\rangle$ by using the density matrix reduced to the central sites $i = 0$ and $i = 1$ (see Fig. 1). In Section 3 it will be shown that the present DMRG algorithm yields accurate results for both global properties including the surface and local bulk-like properties.

For the calculations we take advantage of a theorem by Lieb which states that for $U > 0$ the ground-state spin S of the half-filled Hubbard Hamiltonian on a bipartite lattice is $S = |E_{\rm A} - E_{\rm B}|/2$, where $E_{\rm A}$ and $E_{\rm B}$ are the number of sites belonging to the two sublattices A and B ($N_{\rm a} = E_{\rm A} + E_{\rm B}$ even) [9]. In the Bethe lattice considered in this paper, even and odd shells constitute the two sublattices A and B (NN hopping). At the renormalization iteration ν the ground-state spin is $S = 2^{\nu-1}$ so that the calculations can be performed in the subspace of maximal $S_z = S$. This exact result provides an important simplification that appears to be crucial in order to achieve reliable results with present computer

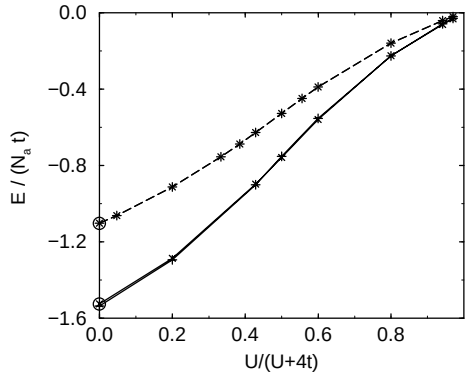

Fig. 3. Ground-state energy per site of the half-filled Hubbard model on a $z = 3$ Bethe lattice as a function of the Coulomb repulsion U/t. The solid curve is calculated locally at the central sites from $E = U\langle\hat{n}_{0\uparrow}\hat{n}_{0\downarrow}\rangle + (zt/2)\sum_\sigma\langle\hat{c}^\dagger_{1\sigma}\hat{c}_{0\sigma} + \hat{c}^\dagger_{0\sigma}\hat{c}_{1\sigma}\rangle$ (see Fig. 1). The dashed curve is the average energy E_s of the complete system including the surface. Crosses (plus signs) correspond to even (odd) renormalization iterations. The corresponding exact results for $U = 0$ are given by the open circles.

facilities, since for $S_z = S$ the Hilbert space is much smaller than for $S_z = 0$. Thus, the number of states m kept in the renormalized blocks can be reduced significantly without loss of accuracy. For example, for $U = 0$, we have performed DMRG calculations by using $S_z = 0$ and $S_z = S$, keeping in both cases $m = 20$ states in the renormalized blocks. After the first few iterations one finds important differences in the ground-state energy per site, the $S_z = 0$ converged results being $2.6 \times 10^{-2}t$ higher than those corresponding to $S_z = S$. Moreover, the sum P_m of the retained eigenvalues of the density matrix — a good criterion to estimate the quality of a DMRG calculation [5] — follows the same trend. Indeed, for $S_z = S$, $1 - P_m$ is always smaller than 7×10^{-4} while for $S_z = 0$, $1 - P_m$ can be as large as 2×10^{-2}, a value that in practice is too large for obtaining reliable results. In addition it should be noted that the uncorrelated limit is the most difficult case in DMRG calculations. $1 - P_m$ is in fact always smaller for finite U/t than for $U = 0$ [11]. The results presented in this paper were obtained for $S_z = S$ by keeping $m = 20$ states in each renormalized block. This would correspond to $4^4m^3 = 2,048,000$ possible configurations. However, only between 100,000–130,000 of them belong to the $S_z = S$ subspace. Still, the dimension of the system-block density-matrix, $16m^2 = 6400$, is quite important, which renders the computations very demanding.

3 Results and discussion

In Figure 3 results are given for the ground-state energy per site as a function of U/t. Since in the Bethe lattice the weight of the atoms close to the surface does not vanish with increasing number of shells, it is necessary to discern between global properties, which include surface contributions, and local properties calculated close to the central site $i = 0$. The global energy E_s (dashed curve) is derived by extrapolating the ground-state energy per site for $L \to \infty$. The effects of truncation to $m = 20$ states per renormalized block can be inferred by comparison with exact results for some limiting cases. For $U = 0$ the DMRG calculations yield $E_\mathrm{s} = -1.102\,68t$, while the exact results obtained by diagonalizing the finite-L tight-binding matrix and extrapolating to $L \to \infty$ is $E_\mathrm{s}^\mathrm{ex} = -1.103\,06t$ (see Appendix). The agreement seems quite remarkable, since E_s is given by the contributions of the atoms of the outermost shells that are renormalized already from the very first iterations. Let us recall that 1/2 of the sites belong to the surface, 1/4 to the layer below the surface, and so on. Similarly good results are obtained for the local ground-state energy per site E (solid curve) which is obtained from the density matrices at the central sites extrapolated for $L \to \infty$. For $U = 0$, we obtain $E = -1.524\,7t$, while the integral of the single-particle density of states of the Bethe lattice is $E^\mathrm{ex} = -1.525\,5t$. The renormalized blocks thus provide a proper embedding of the central sites. It is worth noting that the accuracy of these results, derived by keeping only $m = 20$ states per block and setting $S_z = S$ at each iteration, is comparable to the accuracy of calculations with $m = 100$–150 in the 1D Hubbard model ($S_z = 0$). It goes without saying that $m = 100$ calculations on a Bethe lattice are hardly feasible with present computer facilities. Since the uncorrelated limit is the most difficult (less precise) case in DMRG calculations on the Hubbard model [11], we may expect that the results for finite U/t are at least as accurate. This is also confirmed by the fact that the sum P_m of the retained eigenvalues of the block density-matrix increases with U/t.

E and E_s increase monotonously with U/t and vanish as expected in the Heisenberg limit. Their U/t dependence are very similar. In fact, allowing for a rescaling of the energies at $U = 0$, $E/E(U=0)$ and $E_\mathrm{s}/E_\mathrm{s}(U=0)$ are close to the corresponding results for the 1D Hubbard chain [10]. Quantitatively, E_s is always higher than E due to surface boundary effects. Surface sites at the outermost shell have a smaller local coordination number $z = 1$. Therefore the effective local band width and binding energy of surface sites are smaller than in the bulk.

Several local properties have been calculated around the central site $i = 0$ in order to analyze the behavior of the ground-state in the bulk limit. Results for the average local magnetic moment $\langle\hat{S}_z(0)\rangle$ are shown in Figure 4. $\langle\hat{S}_z(0)\rangle$ increases monotonously with U/t reaching 0.35 in the Heisenberg limit. Moreover, for NN sites ($i = 0$ and $i = 1$) we obtain $\langle\hat{S}_z(1)\rangle \simeq -\langle\hat{S}_z(0)\rangle$ and $\langle\hat{S}_z(1')\rangle \simeq \langle\hat{S}_z(1)\rangle$ ($|\langle\hat{S}_z(0) + \hat{S}_z(1)\rangle| \leq 10^{-4}$). The sign alternation of $\langle\hat{S}_z(i)\rangle$ at sites belonging to different sublattices A and B suggests the existence of strong NN AF correlations, as it shall be discussed in more detail below. Notice that the calculated $\langle\hat{S}_z(0)\rangle$ does not vanish in the uncorrelated limit as it should. From the tight-binding solution for the Bethe lattice with a finite number of shells L one obtains

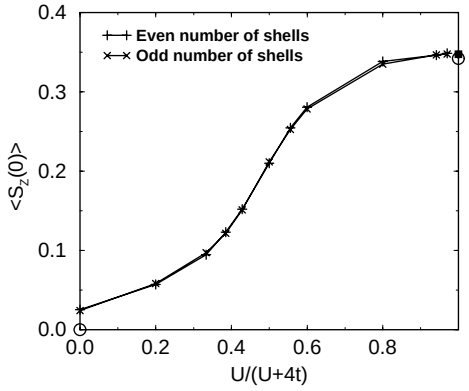

Fig. 4. Average magnetization $\langle \hat{S}_z(0) \rangle$ for the half-filled Hubbard model on a Bethe lattice ($z = 3$) calculated at the central site $i = 0$. Circles indicate tight-binding exact results ($U = 0$) or perturbation theory estimates ($U = \infty$). The filled square ($U = \infty$) is the DMRG result for the Heisenberg model on the $z = 3$ Bethe lattice.

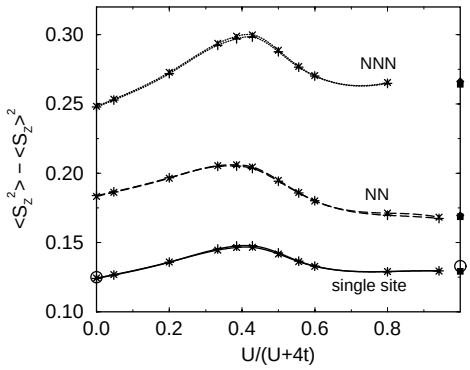

Fig. 5. Bethe-lattice results for the average spin fluctuations $\langle \hat{S}_z^2 \rangle - \langle \hat{S}_z \rangle^2$ as a function U/t, where $\hat{S}_z = \hat{S}_z(0)$ (single site, solid curve), $\hat{S}_z = \hat{S}_z(0) + \hat{S}_z(1)$ (NN spins, dashed curve) and $\hat{S}_z = \hat{S}_z(1) + \hat{S}_z(1')$ (NNN spins, dotted curve). See Figure 1. Circles indicate tight-binding exact results ($U = 0$) or perturbation theory estimates ($U = \infty$). The filled squares (diamonds) for $U = \infty$ show the DMRG results for the Heisenberg model on the $z = 3$ Bethe lattice corresponding to odd (even) iterations.

$\langle \hat{S}_z(0) \rangle = 1/(3L + 2)$ for L even and $\langle \hat{S}_z(0) \rangle = 0$ for L odd (see Appendix). Thus, in finite-size systems with even L the local magnetization does not vanish even for $U = 0$ ($S_z = S$). Our DMRG calculations follow precisely the exact results during the first renormalization iterations but for large ν a slight increase of $\langle \hat{S}_z(0) \rangle$ is observed for L odd which yields a small non-zero value in the extrapolation to $L \to \infty$ ($\langle \hat{S}_z(U=0) \rangle = 0.025$). We therefore expect that this inaccuracy will be remedied by increasing the number of states kept in each renormalized block. In any case, since the DMRG method has better convergence properties with increasing U/t, the precision of the results improves rapidly for finite values of the interaction. In fact, in the strongly correlated limit, the calculated $\langle S_z(0) \rangle = 0.35$ is in very good agreement with perturbative estimations and with DMRG calculations using the Heisenberg Hamiltonian.

Small differences are found in the results for even and odd iterations. These are a consequence of the limited number m of states kept per block and of the fact that the infinite-lattice results are obtained by extrapolation of a succession of finite-system calculations. Even and odd iterations correspond, respectively, to even and odd number of shells L. The properties of finite systems show even-odd oscillations as a function of L, the amplitude of which decreases with increasing number of shells and vanishes for the infinite system. These trends are well reproduced by the DMRG results for finite L. The discrepancies in the extrapolations for even-L and odd-L reflect inaccuracies due to the small number of states m, they are reduced by increasing m. Since the extrapolations to $L = \infty$ are performed independently for even and odd L, the small differences found in the final results show that such discrepancies are not significant (see Fig. 4).

In order to analyze the strongly interacting Heisenberg limit we approximate the ground-state wave function by including first-order perturbations to the Néel state ϕ_0:

$$\psi^{(1)} = \phi_0 - \frac{1}{2(z-1)} \sum_{\langle i,j \rangle} (S_j^+ S_i^- + S_j^- S_i^+) \phi_0 \, . \qquad (3.1)$$

Notice that the coefficient of the first-order correction (spin-flip states) is independent of the exchange constant $J = 4t^2/U$, since the off-diagonal matrix elements $(J/2)$ and the energy differences $\big(2(z-1)J/2\big)$ are both proportional to J in the Heisenberg model. The average of local operators $\hat{O}$ (*e.g.*, $\hat{O} = \hat{S}_z(0)$ or $\hat{O} = \hat{S}_z(0)\hat{S}_z(1)$) are obtained from

$$\langle \hat{O} \rangle = \frac{\mathrm{Tr}[\hat{\rho}\hat{O}]}{\mathrm{Tr}[\hat{\rho}]} \, , \qquad (3.2)$$

where $\hat{\rho}$ refers to the reduced density matrix. For example, for a single site, equation (3.1) yields $\rho(\uparrow,\uparrow) = 1$, $\rho(\downarrow,\downarrow) = 3/16$, and $\rho(\uparrow,\downarrow) = \rho(\downarrow,\uparrow) = 0$. In this way one obtains $\langle \hat{S}_z(i) \rangle = 13/38 = 0.342$, which compares very well with the DMRG result $\langle \hat{S}_z(i) \rangle = 0.348$ for $U/t = 128$. We conclude that the reduction of $\langle \hat{S}_z(i) \rangle$ with respect to the saturation value $1/2$ at very large U/t is the result of quantum spin fluctuations involving mainly the first NN shell of atom i. In addition, we have also performed DMRG calculations for the Heisenberg model on the $z = 3$ Bethe lattice which confirm the Hubbard results at $U/t \gg 1$ ($\langle \hat{S}_z(i) \rangle = 0.347$, see Fig. 4).

In Figure 5 results are given for the fluctuation of the local magnetic moments at a single site and at pairs of NN and NNN sites. In all cases, $\langle S_z^2 \rangle - \langle S_z \rangle^2$ presents a maximum for $U/t = 2.4$–2.9. This behavior is a consequence of the interplay between the reduction of double occupations due to correlations, which increases $\langle S_z^2 \rangle$, and the formation of permanent magnetic moments $\langle S_z \rangle$, which reduces

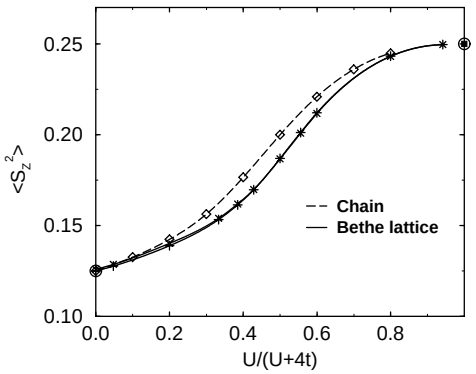

Fig. 6. $\langle \hat{S}_z(0)^2 \rangle$ of the half-filled Hubbard model as a function U/t. The solid curve corresponds to the $z = 3$ Bethe lattice and the dashed curve to the one-dimensional chain ($z = 2$). Circles indicate tight-binding exact results ($U = 0$) or perturbation theory estimates ($U = \infty$). The filled square for $U = \infty$ shows the DMRG result for the Heisenberg model on the $z = 3$ Bethe lattice.

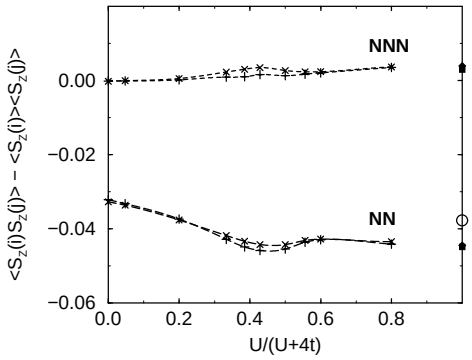

Fig. 7. Spin correlation functions $\langle \hat{S}_z(i)\hat{S}_z(j)\rangle - \langle \hat{S}_z(i)\rangle\langle \hat{S}_z(j)\rangle$ between NN sites and NNN sites. For $U = \infty$, the open circle indicates a perturbation-theory estimate (Eq. (3.1)) and the filled squares (diamonds) show the DMRG results for the Heisenberg model on the $z = 3$ Bethe lattice corresponding to odd (even) iterations.

the fluctuation of the spin moments around their average (see Fig. 4). As shown in Figure 6, $\langle S_z^2 \rangle$ in the Bethe lattice increases monotonously with U/t very much like in the 1D Hubbard chain. The main qualitative difference between Bethe-lattice and 1D results for $\langle S_z^2 \rangle - \langle S_z \rangle^2$ comes from $\langle S_z \rangle$ which is zero for the 1D case. Notice that the DMRG calculations are in good quantitative agreement with the tight-binding analytic results (open circles, $U = 0$), with independent DMRG calculations for the spin-1/2 Heisenberg model (filled squares and diamonds, $U = \infty$), and with the first-order-perturbation estimation from equations (3.1, 3.2) (open circles, $U = \infty$).

The longitudinal spin correlation functions $\gamma_{ij} = \langle \hat{S}_z(i)\hat{S}_z(j)\rangle - \langle \hat{S}_z(i)\rangle\langle \hat{S}_z(j)\rangle$ between NN and NNN sites i and j are given in Figure 7. Notice that γ_{ij} is not proportional to the rotational invariant spin correlation function $\langle \mathbf{S}(i) \cdot \mathbf{S}(j)\rangle - \langle \mathbf{S}(i)\rangle \cdot \langle \mathbf{S}(j)\rangle$ (including the transversal directions) since the calculations were performed in the $S_z = S$ subspace. NN spins show strong AF correlations that are important already for $U = 0$ and that become even stronger as U/t increases. A shallow maximum is observed approximately at the same value of U/t for which $\langle S_z^2 \rangle - \langle S_z \rangle^2$ is maximal. As expected, good agreement is obtained between the Hubbard results for large U/t and independent DMRG calculations for the Heisenberg model. First-order estimates of γ_{ij} derived from equation (3.1) are somewhat less accurate than the corresponding estimates of $\langle \hat{S}_z(0)\rangle$ or $\langle \hat{S}_z^2(0)\rangle$ but they still remain qualitatively correct (see Figs. 4 and 6). The spin correlations between NNN's are much weaker than between NN's. Moreover, in this case parallel alignment is slightly favored as U/t increases ($\langle \hat{S}_z(1)\hat{S}_z(1')\rangle - \langle \hat{S}_z(1)\rangle\langle \hat{S}_z(1')\rangle > 0$). These trends are consistent with the sign alternations in $\langle \hat{S}_z(i)\rangle$ found around the central site for i belonging to different sublattices. The strong AF correlations between NN's may first suggest the possibility of a spin-density-wave instability in the bipartite Bethe lattice. However,

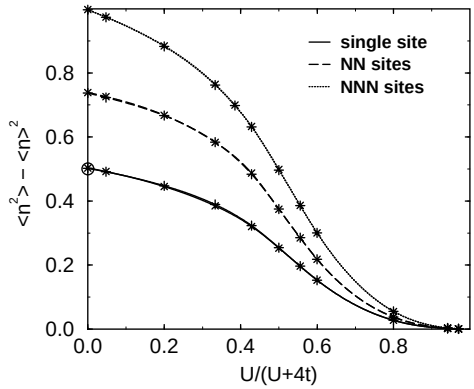

Fig. 8. Bethe-lattice results for the density fluctuations $\langle \hat{n}^2 \rangle - \langle \hat{n} \rangle^2$ as a function U/t, where $\hat{n} = \hat{n}(0)$ (single site, solid curve), $\hat{n} = \hat{n}(0) + \hat{n}(1)$ (NN sites, dashed curve) and $\hat{n} = \hat{n}(1) + \hat{n}(1')$ (NNN sites, dotted curve). $\hat{n}(i) = \hat{n}_{i\uparrow} + \hat{n}_{i\downarrow}$, see Figure 1.

the very small values of the NNN correlations cast doubts on the existence of long-range Néel like order. This more subtle issue cannot be decided on the basis of the computed properties, since this would require a systematic calculation of the long-range spin correlations as a function of distance.

The average density $\langle \hat{n}(i)\rangle$ at the central sites $i = 0$ and $i = 1$ is very close to 1 independently of U/t, which confirms the expected absence of a charge-density wave for $U \geq 0$ ($|\langle \hat{n}_{i\uparrow} + \hat{n}_{i\downarrow}\rangle - 1| < 10^{-4}$). The fluctuations of the density at a single site, and at pairs of NN and NNN sites are given in Figure 8. In all cases we observe a monotonic crossover from the uncorrelated regime ($\langle \hat{n}^2 \rangle - \langle \hat{n} \rangle^2$ maximal) to the strongly correlated, localized regime where charge fluctuations are suppressed. The U/t dependence is quite similar to what is obtained for 1D Hubbard model. The density fluctuation at a pair of NNN sites (dotted curve) is approximately twice the single-site result (solid curve) which indicates, as in the case of the spin degrees of freedom, that density correlations between

NNN's are very weak ($\langle\hat{n}(1)\hat{n}(1')\rangle - \langle\hat{n}(1)\rangle\langle\hat{n}(1')\rangle \simeq 0$). In contrast, for NN sites charge fluctuations are significantly smaller. One observes that $\langle[\hat{n}(0)+\hat{n}(1)]^2\rangle - \langle\hat{n}(0)+\hat{n}(1)\rangle^2 \simeq (3/2)[\langle\hat{n}(0)^2\rangle - \langle\hat{n}(0)\rangle^2]$ or equivalently $\langle\hat{n}(0)\hat{n}(1)\rangle - \langle\hat{n}(0)\rangle\langle\hat{n}(1)\rangle \simeq [\langle\hat{n}(0)^2\rangle - \langle\hat{n}(0)\rangle^2]/2$. Notice that these relations hold approximately for all values of U/t, even for $U=0$. The ratio between single-site charge fluctuations and fluctuations on a pair of NN's is not much affected by changes in the Coulomb repulsion strength. Therefore, this seems to result mainly from the geometrical proximity of NN sites.

4 Conclusion

Several ground-state properties of the half-filled Hubbard model have been determined on the Bethe lattice with coordination $z=3$ by using a density-matrix renormalization group (DMRG) algorithm for open infinite systems. Although the lattice is not one dimensional (1D), the existence of a unique path between any pair of sites allows to formulate a simple renormalization procedure. In contrast to previous density-matrix renormalization studies of Hubbard-like models on 1D chains or ladders, where the number of sites $N_{\rm a}$ increases linearly with the number of iterations ν, $N_{\rm a}$ increases here exponentially with ν ($N_{\rm a} = 3\times 2^{\nu}-2$). This is a consequence of the fact that 2 blocks are renormalized into a single one at each iteration. Despite the very rapid increase of $N_{\rm a}$, the DMRG method provides accurate results over the whole range of U/t already by keeping few states per block ($m=20$). In practice, this is achieved by working in the subspace of maximal spin projection $S_z = S$, where the ground-state spin $S = 2^{\nu-1}$ is derived from a theorem by Lieb [9]. For example, in the limit of $U=0$ the calculated ground-state energy per site differs by only $3\times 10^{-4}t$ from the exact tight-binding result. It is remarkable that this level of precision concerns not only local properties calculated at the unrenormalized central sites, but also global properties which are dominated by the renormalized sites of the outermost shells. From a general point of view, the present study encourages renormalizations of more than one block into a system block in future DMRG algorithms.

The main results for the $z=3$ Bethe lattice may be summarized as follows. The local magnetic moments $\langle\hat{S}_z(i)\rangle$ at the central site $i=0$ and its NN's $i=1$ increase monotonically with U/t showing AF local order among the spin polarizations at sites belonging to different sublattices of the bipartite Bethe lattice ($\langle\hat{S}_z(1)\rangle \simeq -\langle\hat{S}_z(0)\rangle$). The maximum $\langle\hat{S}_z(i)\rangle$ found in the Heisenberg limit ($\langle\hat{S}_z(i)\rangle = 0.35$) is reduced with respect to the saturation value $\langle\hat{S}_z(i)\rangle = 1/2$ as a result of exchange flips between the spin at site i and the spins at its NN's that point in the opposite direction. The fluctuations of the local spins $\langle S_z(i)^2\rangle - \langle S_z(i)\rangle^2$ show a maximum as a function of U/t for $U/t = 2.4$–2.9. For small U/t the usual increase of $\langle S_z(i)^2\rangle$ due to the reduction of double occupations dominates, while for large U/t the formation of large permanent moments $\langle S_z(i)\rangle$ blocks local spin fluctuations. NN sites show strong AF spin correlations that increase with increasing Coulomb repulsion. However, NNN sites are very weakly correlated over the whole range of U/t. The AF correlations seem to be very short ranged in contrast to the static picture of a spin density wave. This reflects the importance of quantum fluctuations in the $z=3$ Bethe lattice as in 1D systems.

Taking into account that the Bethe lattice is one of the standard models for the studying the limit of infinite dimensions, it would be very interesting to compare the present results for $z=3$ with the outcome of the $d=\infty$ equations in order to quantify the importance of $1/d$ corrections. Although there is no intrinsic impediment for applying the method proposed in this paper to $z>3$, it is also true that the computational effort involved in such calculations increases extremely rapidly with z. Systematic DMRG studies for large z seem therefore unfeasible. Still, an extension of the present work to moderately small z (*e.g.*, $z=4$ and $z=5$) should become possible in the near future. In addition, DMRG investigations including NNN hoppings or using the Bethe lattice for embedding a finite cluster should be very valuable, particularly since the information derived from the DMRG method is complementary to finite-temperature quantum Monte-Carlo calculations.

Computer resources provided by IDRIS (CNRS) are gratefully acknowledged.

Appendix

The aim of this section is to outline the block diagonalization of the tight-binding matrix of a *finite* Bethe lattice formed by a central site $i=0$ and L successive nearest neighbor (NN) shells. The number of sites at shell l ($1\le l\le L$) is given by $N_{\rm s}(l) = z(z-1)^{l-1}$, where z refers to the coordination number. The notation used for labeling the lattice sites is illustrated in Figure 9 for $z=3$. A site belonging to the shell l is denoted by the set of l numbers $(i_1, i_2, \ldots i_l)$ which define the path to follow in order to reach the desired site starting from the central site $i=0$. The tight-binding matrix H_0 of the $z=3$ Bethe lattice with NN hoppings t can be block diagonalized by using that the finite Bethe lattice is invariant after the transposition of any pair of branches that connect a site of shell $l-1$ with its 2 NN's of shell l. For the outermost shell ($l=L$) the symmetry adapted single-particle states are

$$|i_1, i_2, \ldots i_{L-1}, +\rangle = \big(|i_1, i_2, \ldots i_{L-1}, 1\rangle + |i_1, i_2, \ldots i_{L-1}, 2\rangle\big)/\sqrt{2} \quad \text{(A.1)}$$

$$|i_1, i_2, \ldots i_{L-1}, -\rangle = \big(|i_1, i_2, \ldots i_{L-1}, 1\rangle - |i_1, i_2, \ldots i_{L-1}, 2\rangle\big)/\sqrt{2}. \quad \text{(A.2)}$$

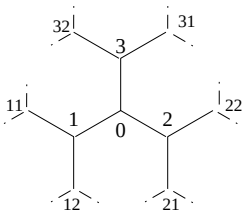

Fig. 9. Labeling of Bethe-lattice sites used in this appendix.

For the other shells ($l < L$) one proceeds recursively in the same way building symmetric and antisymmetric linear combinations. For the first shell the 3-fold symmetry around the central site $i = 0$ is applied.

In the new basis H_0 splits in a $(L+1)\times(L+1)$ matrix block of the form

$$A = \begin{bmatrix} 0 & \sqrt{3}t & 0 & & \cdots & \\ \sqrt{3}t & 0 & \sqrt{2}t & 0 & & \\ 0 & \sqrt{2}t & 0 & \sqrt{2}t & & \\ \vdots & & \ddots & \ddots & \ddots & \\ & & & & & \sqrt{2}t \\ & & & & \sqrt{2}t & 0 \end{bmatrix}, \qquad \text{(A.3)}$$

that involves only purely even states including the central site, and in smaller $l \times l$ matrices B_l with $1 \le l \le L$ of the form

$$B_l = \begin{bmatrix} 0 & \sqrt{2}t & 0 & & \cdots & \\ \sqrt{2}t & 0 & \sqrt{2}t & 0 & & \\ 0 & \sqrt{2}t & 0 & \sqrt{2}t & & \\ \vdots & & \ddots & \ddots & \ddots & \\ & & & & & \sqrt{2}t \\ & & & & \sqrt{2}t & 0 \end{bmatrix}. \qquad \text{(A.4)}$$

B_L appears twice in H_0, and each of the other B_l appears $3 \times 2^{L-l-1}$ instances in the total tight-binding matrix.

The eigenvalues of B_l are $\beta_k = -2\sqrt{2}t \cos\frac{k\pi}{l+1}$ with $k \in [1, l]$, and those of A are $\alpha_k = -2\sqrt{2}|t| \cos\theta_k$, where the θ_k are the roots of $2\sin(L+2)\theta = \sin L\theta$. The later equation is solved numerically and the tight-binding energy per site E_s of the finite Bethe lattice is determined for any L.

The extrapolated value for $L \to \infty$ is $E_s = -1.10306t$. Notice that this result differs from the integral of the local density of states at the central site ($E = -1.5255t$), since $E_s(L \to \infty)$ is dominated by surface contributions.

References

1. W. Metzner, D. Vollhardt, Phys. Rev. lett. **62**, 324 (1989); D. Vollhardt, in *Correlated Electron Systems,* edited by V.J. Emery (World Scientific, Singapore, 1993).
2. M.J. Rozenberg, X.Y. Zhang, G. Kotliar, Phys. Rev. Lett. **69**, 1236 (1992); M.J. Rozenberg, G. Kotliar, X.Y. Zhang, Phys. Rev. B **49**, 10181 (1994).
3. A. Georges, W. Krauth, Phys. Rev. Lett. **69**, 1240 (1992); Phys. Rev. B **48**, 7167 (1993).
4. J. Hong, H.Y. Kee, Phys. Rev. B **52**, 2415 (1995).
5. S.R. White, Phys. Rev. Lett. **69**, 2863 (1992); Phys. Rev. B **48**, 10345 (1993).
6. S.R. White, D.A. Huse, Phys. Rev. B **48**, 3844 (1993); K.A. Hallberg, P. Horsh, G. Martinez, Phys. Rev. B **52**, R719 (1995); S.R. White, Phys. Rev. B **53**, 52 (1996); S. Liang, H. Pang, Europhys. Lett. **32**, 173 (1995); S. Qin, S. Liang, Z. Su, L. Yu, Phys. Rev. B **52**, R5475 (1995); B. Srinivasan, S. Ramasessha, H.R. Krishnamurthy, Phys. Rev. B **54**, 2276 (1996); H. Pang, S. Liang, Phys. Rev. B **51**, 10287 (1995); S.R. White, Phys. Rev. Lett. **69**, 2863 (1992); C.C. Yu, S.R. White, Phys. Rev. Lett. **71**, 3866 (1993); M. Guerrero, C.C. Yu, Phys. Rev. B **51**, 10301 (1995); M.-B. Lepetit, G.M. Pastor, Phys. Rev. B **58**, 12691 (1998).
7. H. Otsuka, Phys. Rev. B **53**, 14004 (1996); B. Friedman, J. Phys. Cond. Matter **9**, 9021 (1997).
8. J. Hubbard, Proc. R. Soc. London A **276**, 238 (1963); A **281**, 401 (1964); J. Kanamori, Prog. Theo. Phys. **30**, 275 (1963); M.C. Gutzwiller, Phys. Rev. Lett. **10**, 159 (1963).
9. E.H. Lieb, Phys. Rev. Lett. **62**, 1201 (1989).
10. E.H. Lieb, F.Y. Wu, Phys. Rev. Lett. **20**, 1445 (1968).
11. M.-B. Lepetit, G.M. Pastor, Phys. Rev. B **56**, 4447 (1997).